Fluid Phase Equilibria 393 (2015) 85–90

Contents lists available at ScienceDirect

Fluid Phase Equilibria

journal homepage: www.elsevier.com/locate/fluid

Structural transition and phase behavior of N_2 gas hydrates with pinacolyl alcohol and *tert*-amyl alcohol

Eunae Kim [a], Young Keun Jin [b], Yongwon Seo [a,*]

[a] School of Urban and Environmental Engineering, Ulsan National Institute of Science and Technology, Ulsan 689-798, Republic of Korea
[b] Division of Polar Earth-System Sciences, Korea Polar Research Institute, Incheon 406-840, Republic of Korea

ARTICLE INFO

Article history:
Received 3 December 2014
Received in revised form 26 February 2015
Accepted 27 February 2015
Available online 27 February 2015

Keywords:
Pinacolyl alcohol
tert-Amyl alcohol
Nitrogen
sH hydrate
Structural transition

ABSTRACT

The influences of large molecular alcohols (LMAs) (pinacolyl alcohol (PCA) and *tert*-amyl alcohol (tAA)) on N_2 hydrate were examined with a primary focus on the hydrate phase equilibria and structural transition. The four-phase ($H–L_w–L_{LMA}–V$) equilibria of the N_2 + PCA + water and N_2 + tAA + water systems were experimentally measured in order to determine the thermodynamic stability conditions of the N_2 hydrates with LMAs. The $H–L_w–L_{LMA}–V$ curves of both N_2 + PCA and N_2 + tAA hydrates were significantly shifted to more thermodynamically stable regions. Powder X-ray diffraction (PXRD) and Raman analyses verified that the structure of N_2 hydrates with LMAs was transformed from the original structure of sII to sH (*P6/mmm*) as a result of the inclusion of LMAs. In addition, the formation of sH hydrate from the N_2 + PCA + water system was further verified using an endothermic dissociation thermogram from a high pressure micro-differential scanning calorimeter (HP μ-DSC) by confirming the appearance of three distinct peaks that correspond to ice, sII hydrate, and sH hydrate. Therefore, the experimental results that were obtained in this study are expected to be informative for understanding the roles of LMAs in affecting the macroscopic hydrate phase behavior and microscopic hydrate structure.

1. Introduction

Clathrate hydrates are non-crystalline compounds that consist of water molecules (host molecules) and guest molecules [1]. Water molecules create cages by forming hydrogen bonds, and guest molecules are enclathrated in those cages and stabilize the clathrate hydrates. There are various applications of clathrate hydrates, such as carbon dioxide capture and storage, natural gas storage/transportation, and desalination [2–14]. The structures of clathrate hydrates are generally determined by the sizes of guest molecules and the most common three structures are sI, sII and sH. sI hydrates consist of two small (5^{12}) cages and six large ($5^{12}6^2$) cages, sII hydrates consist of sixteen small (5^{12}) cages and eight large ($5^{12}6^4$) cages, and sH hydrates consist of three small (5^{12}) cages, two medium ($4^35^66^3$) cages, and one large ($5^{12}6^8$) cage [1].

Among these three structures, sH hydrates have several noteworthy features regarding thermodynamics and their potential applications. First, in the presence of small-sized help gases, sH hydrates are capable of capturing large-sized liquid hydrocarbon guests, which cannot be enclathrated in the lattices of sI or sII hydrates. Second, sH hydrates have a higher gas storage potential in their smaller cages (5^{12} and $4^35^66^3$) compared to sI and sII hydrates when the larger cages of each structure are assumed to be occupied by large molecules. Last, by enclathrating large molecular guests, sH hydrates generally become more stabilized than their original thermodynamic conditions [15,16].

Neohexane and methylcyclohexane among large-sized liquid hydrocarbons are well-known sH guests that fill the large ($5^{12}6^8$) cages in the presence of help gases such as CH_4, Xe, and H_2S that fill the small (5^{12}) and medium ($4^35^66^3$) cages, and have been extensively investigated due to their thermodynamic promoting ability [17–19]. However, large molecular alcohols (LMAs) have not been examined thoroughly as sH hydrate guests, although they are expected to be enclathrated in the large ($5^{12}6^8$) cages of sH hydrates [20]. Furthermore, N_2 has rarely been used as a help gas of sH hydrates despite its appropriate molecular size for enclathration in the small (5^{12}) and medium ($4^35^66^3$) cages of sH hydrates [21,22]. For these reasons, the enclathration of LMAs in sH hydrates in the presence of N_2 as a help gas needs to be investigated.

In this study, pinacolyl alcohol (PCA) and *tert*-amyl alcohol (tAA), which have six and five carbons respectively, were selected as representative LMAs. N_2 was chosen as a help gas for the sH hydrate formation because N_2 itself can form sII hydrate, whereas LMAs such as PCA and tAA cannot form any clathrate hydrates by

* Corresponding author. Tel.: +82 52 217 2821; fax: +82 52 217 2819.
E-mail address: ywseo@unist.ac.kr (Y. Seo).

http://dx.doi.org/10.1016/j.fluid.2015.02.033
0378-3812/

Table 1
Source and purity of the materials used in this study.

Chemical Name	Source	Purity
N_2	PSG gas	0.9999
PCA[a]	Sigma–Aldrich	0.98
tAA[b]	Sigma–Aldrich	0.99

[a] PCA: pinacolyl alcohol (3,3-dimethyl-2-butanol).
[b] tAA: *tert*-amyl alcohol (2-methyl-2-butanol).

themselves. The four-phase (H (hydrate)–L_w (liquid water)–L_{LMA} (liquid large molecular alcohol)–V (vapor)) equilibria of the N_2 + PCA + water and N_2 + tAA + water systems were experimentally measured in order to determine the thermodynamic stability conditions of the N_2 hydrates with LMAs. To confirm the possible structural transitions due to the enclathration of the LMAs, both the N_2 + PCA and N_2 + tAA hydrates were analyzed using powder X-ray diffraction (PXRD) and Raman spectroscopy. In addition, additional verification of the sH hydrate formation from the N_2 + PCA + water system was obtained using an endothermic dissociation thermogram from a high pressure micro-differential scanning calorimeter (HP μ-DSC).

2. Experimental

2.1. Materials and apparatus

N_2 gas with a purity of 99.99% was supplied by PSG Gas Co. (Republic of Korea). Pinacolyl alcohol with 98% purity and *tert*-amyl alcohol with 99% purity were purchased from Sigma–Aldrich (USA). The suppliers and purity of the materials used in this experiment are presented in Table 1. Double distilled, deionized water was used. All materials were used without further purification.

The experimental apparatus used in this study was specifically manufactured to accurately measure the changes in the pressure and temperature of the hydrate formation and dissociation process. The equilibrium cell was made of 316 stainless steel with an internal volume of 250 cm^3, and it was immersed in a water bath that was connected to an external circulator with a programmable temperature controller (RW-2025G, JEIO Tech, Republic of Korea). The content in the cell was vigorously agitated by an impeller-type stirrer. A thermocouple with a temperature range from 73.15 to 1273.15 K was introduced into the equilibrium cell to measure the temperature of the cell content. This thermocouple was calibrated using an ASTM 63C mercury thermometer (Ever Ready

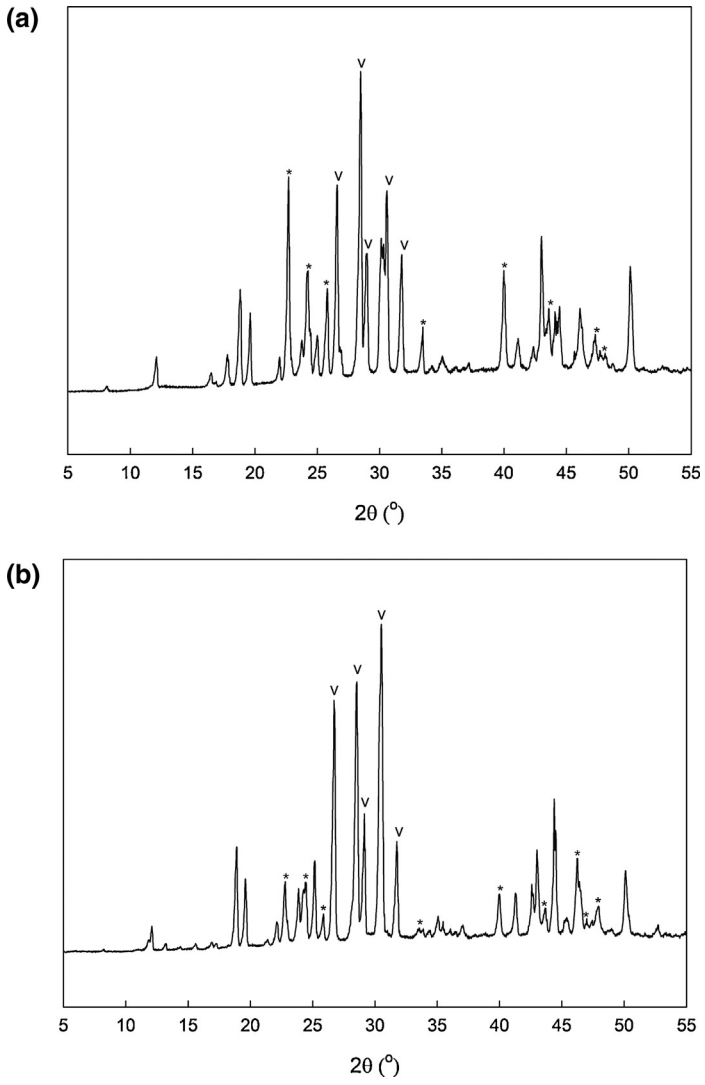

Fig. 1. (a) PXRD patterns of the N_2 + PCA (3.0 mol%) hydrate, (b) PXRD patterns of the N_2 + tAA (3.0 mol%) hydrate. *: Hexagonal ice, v: representative sH peaks.

Thermometer, USA) with a resolution of ±0.1 K. In order to measure the pressure of the system, a pressure transducer (S-10, Wika, Germany) was used. This pressure transducer was calibrated with Heise Bourdon tube pressure gauge (CMM-140830, 0–20.0 MPa, maximum error of ±0.02 MPa).

2.2. Microscopic analyses

For accurate structure identification of the N_2 + LMA hydrates, each gas hydrate sample with LMAs was formed at temperature and pressure conditions where the N_2 + LMA hydrate is stable, but the pure N_2 hydrate is unstable: the N_2 + PCA hydrate was sampled at 278 K and 18.0 MPa, and the N_2 + tAA hydrate was sampled at 275.5 K and 18.5 MPa.

The crystal structures of the N_2 + PCA and N_2 + tAA hydrates were determined using powder X-ray diffraction (PXRD). To obtain the PXRD patterns of the hydrate samples, an X-ray diffractometer (D/Max-RB, Rigaku, Japan) equipped with a graphite-monochromatized Cu Kα1 radiation source (λ = 1.5406 Å) was used. The PXRD patterns were collected stepwise with a fixed time interval of 3 s and a step size of 0.02° for 2θ = 5–55° at 133.15 K. The obtained patterns were analyzed using the CheckCell program.

For Raman measurements, the pure N_2, N_2 + PCA, and N_2 + tAA hydrate samples were finely powdered in a vessel with liquid N_2, and then pelletized into a cylinder with a diameter of 1.0 cm and a height of 0.3 cm. The Raman spectra for each hydrate sample were obtained using a Raman spectrometer (alpha 300R, WITech, Germany) that was equipped with a 1800 grooves/mm holographic grating and a thermoelectrically cooled CCD detector under atmospheric pressure. The excitation source was a He–Ne laser with a wavelength of 532 nm and a laser intensity of 20 mW. The temperature of the sample during the measurement was maintained constant at 170 K by controlling the flow of liquid N_2 vapor.

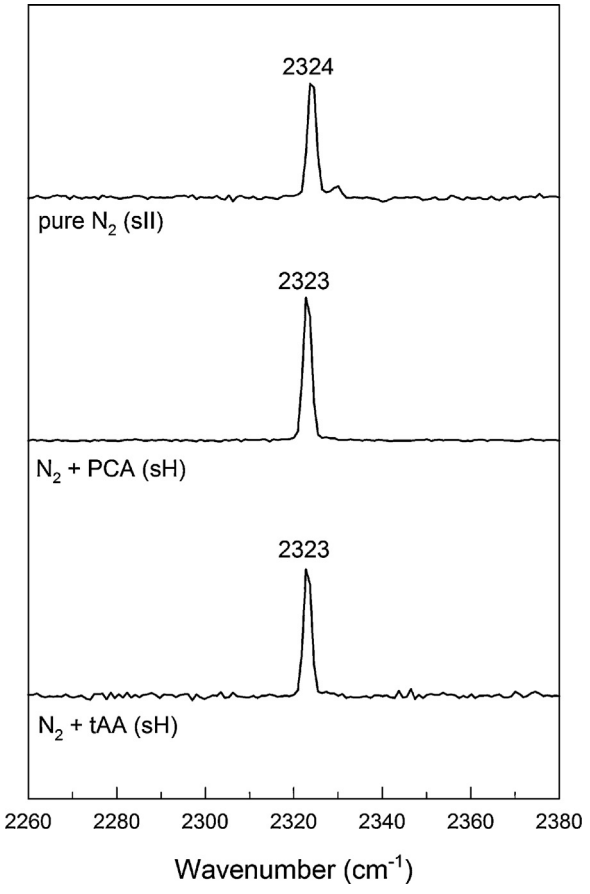

Fig. 2. Raman spectra of the pure N_2, N_2 + PCA (3.0 mol%) and N_2 + tAA (3.0 mol%) hydrates.

2.3. Differential scanning calorimetry

To confirm the formation of the sH hydrate from the N_2 + PCA + water system, a high pressure micro-differential scanning calorimeter (HP μ-DSC, VII Evo Setaram Inc., France) was used. The HP μ-DSC operates in a temperature range of 233.15–393.15 K and a pressure range up to 40 MPa, with a resolution of 0.02 μW and a temperature deviation of ±0.2 K. The multi-cycle mode of cooling and heating between 253 K and 274 K was adopted for approximately 25 mg of PCA solution (3.0 mol%) with N_2 gas at the desired pressure in order to enhance the conversion of the PCA solution into sH hydrates. However, in order to observe all possible phases including ice, sII hydrate, and sH hydrate, the complete conversion to sH hydrate that can be achieved using a large number of cooling–heating cycles was not performed. After 10 cooling–heating cycles, the system was heated from 253 K to 313 K at a rate of 1.0 K/min, and the final endothermic dissociation thermogram was obtained.

2.4. Hydrate stability condition measurements

Pinacolyl alcohol (PCA) and *tert*-amyl alocohol (tAA) are both immiscible with water. Thus, in the four-phase equilibrium system (H–L_w–L_{LMA}–V), there are three components (N_2, water, and LMA) and four phases (gas hydrate (H), liquid water (L_W), liquid alcohol (L_{LMA}), and vapor (V)). According to Gibb's phase rule (F = C–P + 2), the degree of freedom is 1. Therefore, the H–L_w–L_{LMA}–V equilibria of the N_2 + PCA (or tAA) + water systems were independent of the PCA or tAA concentrations. For this reason, all experiments were conducted with 3.0 mol% LMA solutions.

To measure the hydrate-phase equilibria, the equilibrium cell was filled with approximately 80 cm^3 of PCA (3.0 mol%) or tAA (3.0 mol%) solution. Before starting the experiment, the equilibrium cell was ventilated at least three times with N_2 gas to remove any residual air in the equilibrium cell. Then, the equilibrium cell was pressurized with N_2 gas to the desired pressure, and the experiment was conducted under an isochoric condition with stepwise heating/cooling. The whole system was slowly cooled by

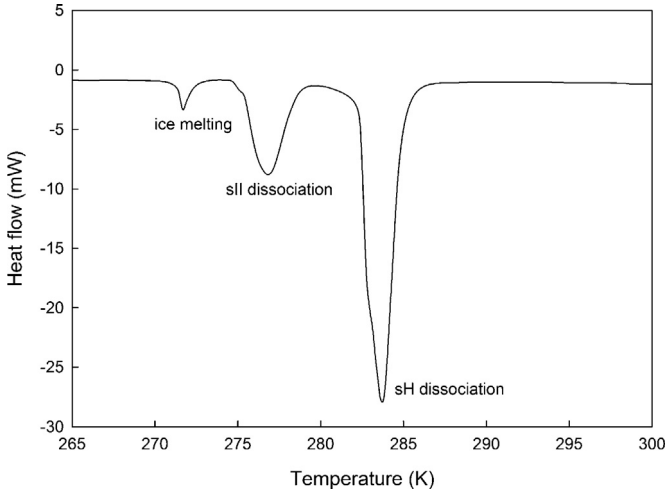

Fig. 3. Dissociation thermogram of the N_2 + PCA (3.0 mol%) hydrate around 20.0 MPa with a heating rate of 1.0 K/min.

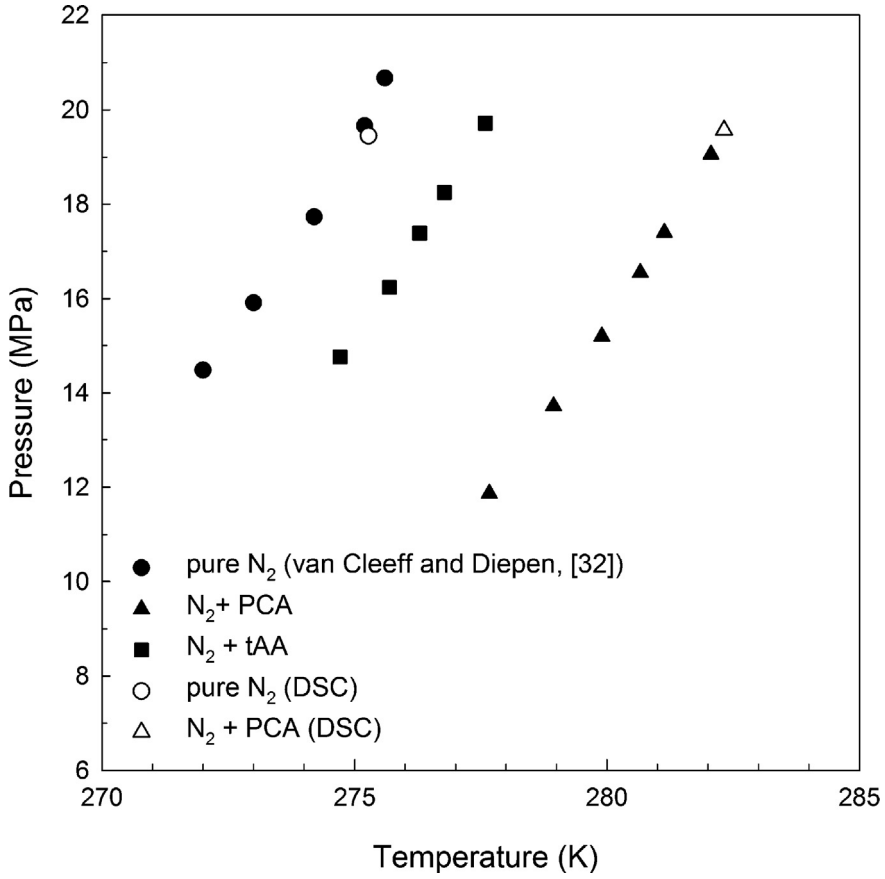

Fig. 4. Phase equilibria of the pure N_2, N_2 + PCA (3.0 mol%) and N_2 + tAA (3.0 mol%) hydrates.

1.0 K/h until the hydrate nucleation began. During this process, there was gradual pressure decrement caused by the thermal contraction until a rapid pressure drop caused by the hydrate nucleation was observed. After sufficient time for the completion of gas hydrate formation, the temperature was slowly increased in a stepwise manner of 0.1 K/90 min. The cell pressure was increased with the hydrate dissociation. Even after the hydrate was completely dissociated, the cell pressure was slightly increased due to the thermal expansion of vapor phase. The intersection point between the hydrate dissociation line and the thermal expansion line was determined as an H–L_w–L_{LMA}–V equilibrium point at each given pressure. More detailed descriptions of the experimental procedure were provided in our previous papers [23–26].

3. Results and discussions

3.1. PXRD analyses of the N_2 + PCA and the N_2 + tAA hydrates

Fig. 1(a) and (b) present the PXRD patterns of the N_2 + PCA (3.0 mol%) and N_2 + tAA (3.0 mol%) hydrates, respectively. The sI, sII, and sH gas hydrates have their own unique X-ray diffraction patterns depending on their crystal structure types. As depicted in Fig. 1(a) and (b), both N_2 + PCA and N_2 + tAA hydrates exhibited five unique diffraction peaks of sH hydrates, which are marked as 'v'. Those five peaks at $2\theta = 26.8^\circ$, 28.5°, 29.3°, 30.5°, and 31.6° are in good agreement with the unique peaks of sH hydrate represented by the CH_4 + methylcyclohexane hydrate, which were reported by Jin et al. [27]. The crystal structures of both N_2 + PCA and N_2 + tAA hydrates were identified to be sH ($P6/mmm$) with unit cell parameters of $a = b = 12.23$ Å and $c = 10.09$ Å, and $a = b = 12.20$ Å and $c = 10.23$ Å, respectively. Considering the crystal structure of the formed hydrates and the molecular sizes of PCA and tAA, both PCA and tAA are expected to be enclathrated in the large ($5^{12}6^8$) cages of the sH hydrate and thus induce a structural transition of the N_2 hydrates from sII to sH.

3.2. Raman analyses of N_2 + PCA and N_2 + tAA Hydrates

Fig. 2 presents a stacked plot of the Raman spectra for the pure N_2, N_2 + PCA (3.0 mol%), and N_2 + tAA (3.0 mol%) hydrates. Even though the N_2 molecules are captured in both small (5^{12}) and large ($5^{12}6^4$) cages of the sII hydrate, the N_2 hydrate exhibits only one Raman peak at 2324 cm^{-1}, which is originated from the N—N vibrational mode of the N_2 molecules captured in both small (5^{12}) and large ($5^{12}6^4$) cages of the sII hydrate [28–30]. The Raman spectrometers with a resolution of 0.5–1.0 cm^{-1}/pixel cannot elucidate peak splits for the N_2 molecules captured in small (5^{12}) and large ($5^{12}6^4$) cages of sII hydrate because the N_2 molecules are too small to be distinguishable in the two different cages of the sII hydrate. However, both N_2 + PCA and N_2 + tAA hydrates exhibit one Raman peak at 2323 cm^{-1}, which indicates a slight wavenumber shift caused by a structural transition.

3.3. Hydrate dissociation thermogram of the N_2 + PCA + water system

To confirm the nucleation and formation of the sH hydrate from the N_2 + PCA + water system, a hydrate dissociation thermogram was obtained using an HP μ-DSC. The HP μ-DSC can measure accurate dissociation enthalpies of gas hydrates and can

Table 2
Experimental (H–L_w–L_{LMA}–V) equilibrium data for temperature T and pressure p, for the N_2 + PCA and N_2 + tAA systems.[a]

N_2 + PCA		N_2 + tAA	
T (K)	p (MPa)	T (K)	p (MPa)
277.7	11.87	274.7	14.76
278.9	13.72	275.7	16.24
279.9	15.20	276.3	17.39
280.7	16.55	276.8	18.25
281.1	17.40	277.6	19.72
282.1	19.06		
282.3	19.57 (DSC)		

[a] Standard uncertainties u are $u(T) = 0.1$ K and $u(p) = 0.02$ MPa.

also provide reliable hydrate phase equilibrium points [25,26,31]. The onset temperature obtained from the hydrate dissociation thermogram was taken as the equilibrium dissociation temperature at a given pressure. In order to measure the dissociation enthalpy of each gas hydrate, a multi-cycle mode of cooling and heating is generally adopted to enhance and maximize the conversion of water into gas hydrates. However, in this study, after only 10 cycles of cooling and heating, the temperature was raised to 313 K at a rate of 1.0 K/min to obtain the hydrate dissociation thermogram including ice, sII hydrate, and sH hydrate.

As seen in Fig. 3, which presents the hydrate dissociation thermogram of the N_2 + PCA + water system, three distinct endothermic peaks of ice, sII hydrate, and sH hydrate were clearly observed. The first endothermic peak with an onset temperature of 271.5 K corresponds to the ice melting; the second peak with an onset temperature of 275.3 K denotes the pure N_2 hydrate (sII) dissociation; and the last large peak with an onset temperature of 282.3 K indicates the N_2 + PCA hydrate (sH) dissociation at 19.57 MPa. Through the endothermic hydrate dissociation thermogram, the formation of sH hydrate from the N_2 + PCA + water system was further clarified.

3.4. Four-phase equilibria of the N_2 + PCA (or tAA) + water system

The four-phase hydrate equilibrium (H–L_W–L_{LMA}–V) curves of the N_2 + PCA + water and N_2 + tAA + water systems were measured in a temperature range of 270–285 K and a pressure range of 10–22 MPa; the results are presented in Fig. 4 and Table 2, respectively. In Fig. 4, the equilibrium data of the pure N_2 hydrate observed by van Cleeff and Diepen [32] are also plotted for comparison. For the N_2 + PCA (or tAA) + water systems, the structural transition from sII to sH as a result of the inclusion of PCA or tAA in the lattices of the N_2 hydrate was expected from the PXRD and Raman analyses. When compared with the pure N_2 hydrate, the equilibrium curves of both N_2 + PCA and N_2 + tAA hydrates were shifted to more stable regions that are represented by higher temperature ranges at any given pressure or lower pressure ranges at any given temperature, which again indicates a clear structural transition due to the enclathration of PCA or tAA. The N_2 + PCA hydrate exhibited a more remarkable equilibrium curve shift to the stable region than the N_2 + tAA hydrate. This might be attributed to the larger molecular size and better molecular configuration of PCA for enclathration in the large ($5^{12}6^8$) cages, which results in the enhanced thermodynamic stability of the sH hydrate.

Furthermore, for the pure N_2 hydrate (sII) and N_2 + PCA hydrate (sH), each onset temperature obtained from each dissociation thermogram at a given pressure was in a good agreement with the hydrate equilibrium data obtained from the conventional isochoric method as shown in Fig. 4, which verifies the reliability of these experiments.

4. Conclusions

In this work, the influences of pinacolyl alcohol (PCA) and *tert*-amyl alcohol (tAA) on the structural transition and hydrate phase behavior of N_2 hydrates were investigated with a primary focus on the microscopic analyses and H–L_w–L_{LMA}–V equilibrium measurements. From the PXRD and Raman spectra, both N_2 + PCA and N_2 + tAA hydrates were identified to be sH hydrates, which indicates a structural transition from the original sII N_2 hydrate. For both N_2 + PCA and N_2 + tAA hydrates, a significant thermodynamic promotion was observed as a result of the inclusion of the PCA and tAA molecules in the hydrate lattices. In addition, in order to further confirm the formation of the sH hydrate, the hydrate dissociation thermogram of the N_2 + PCA + water system was obtained using a HP μ-DSC. The dissociation thermogram clearly demonstrated three distinct peaks representing ice, pure N_2 hydrate (sII), and N_2 + PCA hydrate (sH). Through the overall experimental results obtained in this study, it was found that both PCA and tAA are sH hydrate formers in the presence of N_2 as a help gas.

Acknowledgements

This research was supported by the Korea Polar Research Institute (KOPRI, Grant No. PE14061) and also by Mid-Career Research Program through the National Research Foundation of Korea(NRF) founded by the Ministry of Science, ICT & Future Planning(NRF-2014R1A2A1A11049950).

References

[1] E.D. Sloan, C.A. Koh, Clathrate hydrates of natural gases, third ed., CRC Press, Boca Raton, 2008.
[2] E.D. Sloan, Fundamental principles and applications of natural gas hydrates, Nature 426 (2003) 353–363.
[3] J.S. Gudmundsson, M. Parlaktuna, A.A. Khokhar, Storage of natural gas as frozen hydrate, SPE Prod. Eng. 9 (1994) 69–73.
[4] Y. Seo, S. Lee, I. Cha, J.D. Lee, H. Lee, Phase equilibria and thermodynamic modeling of ethane and propane hydrates in porous silica gels, J. Phys. Chem. B 113 (2009) 5487–5492.
[5] H. Tajima, A. Yamasaki, F. Kiyono, Energy consumption estimation for greenhouse gas separation processes by clathrate hydrate formation, Energy 29 (2004) 1713–1729.
[6] P. Linga, R. Kumar, P. Englezos, The clathrate hydrate process for post and pre-combustion capture of carbon dioxide, J. Hazard. Mater. 149 (2007) 625–629.
[7] A. Adeyemo, R. Kumar, P. Linga, J.A. Ripmeester, P. Englezos, Capture of carbon dioxide from flue or fuel gas mixtures by clathrate crystallization in a silica gel column, Int. J. Greenhouse Gas Control 4 (2010) 478–485.
[8] A. Eslamimanesh, A.H. Mohammadi, D. Richon, P. Naidoo, D. Ramjugernath, Application of gas hydrate formation in separation processes: a review of experimental studies, J. Chem. Thermodyn. 46 (2012) 61–71.
[9] S. Park, S. Lee, Y. Lee, Y. Lee, Y. Seo, Hydrate-based pre-combustion capture of carbon dioxide in the presence of a thermodynamic promoter and porous silica gels, Int. J. Greenhouse Gas Control 14 (2013) 193–199.
[10] S. Park, S. Lee, Y. Lee, Y. Seo, CO_2 capture from fuel gas mixture using semiclathrate hydrates formed by quaternary ammonium salts, Environ. Sci. Technol. 47 (2013) 7571–7577.
[11] H. Lee, Y. Seo, Y.T. Seo, I.L. Moudrakovski, J.A. Ripmeester, Recovering methane from solid methane hydrate with carbon dioxide, Angew. Chem. Int. Ed. 42 (2003) 5048–5051.
[12] Y. Park, D.Y. Kim, J.W. Lee, D.G. Huh, K.P. Park, J. Lee, H. Lee, Sequestering carbon dioxide into complex structures of naturally occurring gas hydrates, Proc. Natl. Acad. Sci. U. S. A. 103 (2006) 12690–12694.
[13] J.H. Cha, Y. Seol, Increasing gas hydrate formation temperature for desalination of high salinity produced water with secondary guests, ACS Sustainable Chem. Eng. 1 (2013) 1218–1224.
[14] K.C. Kang, P. Linga, K. Park, S.J. Choi, J.D. Lee, Seawater desalination by gas hydrate process and removal characteristics of dissolved ions (Na^+, K^+ Mg^{2+}, Ca^{2+}, B^{3+}, Cl^-, SO_4^{2-}), Desalination 353 (2014) 84–90.
[15] A.A. Khokhar, J.S. Gudmundsson, E.D Sloan. Gas storage in structure H hydrates, Fluid Phase Equilib. 150-151 (1998) 383–392.
[16] J.A. Ripmeester, S.T. John, C.I. Ratcliffe, B.M. Powell, A new clathrate hydrate structure, Nature 325 (1987) 135–136.
[17] S. Takeya, A. Hori, T. Uchida, R. Ohmura, Crystal lattice size and stability of type H clathrate hydrates with various large-molecule guest substances, J. Phys. Chem. B 110 (2006) 12943–12947.
[18] A.P. Mehta, E.D. Sloan, Structure H hydrate phase equilibria of methane+liquid hydrocarbon mixtures, J. Chem. Eng. Data 38 (1993) 580–582.

[19] K.A. Udachin, C.I. Ratcliffe, G.D. Enright, J.A. Ripmeester, Structure H hydrate: a single crystal diffraction study of 2,2-dimethylpentane·5(Xe, H_2S)·34H_2O, Supramol. Chem. 8 (1997) 173–176.
[20] R. Ohmura, T. Uchida, S. Takeya, J. Nagao, H. Minagawa, T. Ebinuma, H. Narita, Phase eqeulibrium for structure-H hydrates formed with methane and either pinacolone (3,3-dimethyl-2-butanone) or pinacolyl alcohol (3,3-dimethyl-2-butanol), J. Chem. Eng. Data 48 (2003) 1337–1340.
[21] A. Khan, Stabilization of hydrate structure H by N_2 and CH_4 molecules in $4^3 5^6 6^3$ and 5^{12} cavities, and fused structure formation with $5^{12}6^8$ cage: a theoretical study, J. Phys. Chem. A 105 (2001) 7429–7434.
[22] A. Danesh, B. Tohidi, R.W. Burgass, A.C. Todd, Hydrate equilibrium data of methyl cyclo-pentane with methane or nitrogen, Chem. Eng. Res. Des. 72 (1994) 197–200.
[23] I. Cha, S. Lee, J.D. Lee, G.W. Lee, Y. Seo, Separation of SF_6 from gas mixtures using gas hydrate formation, Environ. Sci. Technol. 44 (2010) 6117–6122.
[24] Y. Seo, H. Lee, Phase behavior and structure identification of the mixed chlorinated hydrocarbon clathrate hydrates, J. Phys. Chem. B 106 (2002) 9668–9673.
[25] S. Lee, Y. Lee, J. Lee, H. Lee, Y. Seo, Experimental verification of methane-carbon dioxide replacement in natural gas hydrates using a differential scanning calorimeter, Environ. Sci. Technol. 47 (2013) 13184–13190.
[26] Y. Lee, S. Lee, J. Lee, Y. Seo, Structure identification and dissociation enthalpy measurements of the $CO_2 + N_2$ hydrates for their application to CO_2 capture and storage, Chem. Eng. J. 246 (2013) 20–26.
[27] Y. Jin, M. Kida, J. Nagao, Structure H (sH) clathrate hydrate with new large molecule guest substances, J. Phys. Chem. C 117 (2013) 23469–23475.
[28] S. Sasaki, S. Hori, T. Kume, H. Shimizu, Microscopic observation and in situ Raman scattering studies on high-pressure phase transformations of a synthetic nitrogen hydrate, J. Chem. Phys. 118 (2003) 7892–7897.
[29] E.P.V. Klaveren, J.P.J. Michels, J.A. Schouten, D.D. Klug, J.S. Tse, Molecular dynamics simulation study of the properties of doubly occupied N_2 clathrate hydrates, J. Chem. Phys. 115 (2001) 10500–10508.
[30] S. Horikawa, H. Itoh, J. Tabata, K. Kawamura, T. Hondoh, Dynamic behavior of diatomic guest molecules in clathrate hydrate structure II, J. Phys. Chem. B 101 (1997) 6190–6192.
[31] M. Kharrat, D. Dalmazzone, Experimental determination of stability conditions of methane hydrate in aqueous calcium chloride solutions using high pressure differential scanning calorimetry, J. Chem. Thermodyn. 35 (2003) 1489–1505.
[32] A. van Cleeff, G.A.M. Diepen, Gas hydrates of nitrogen and oxygen. II, Recl. Trav. Chim. Pays-Bas 84 (1965) 1085–1093.